

Observation of Completely Destructive Quantum Interference between Interacting Resonances in Molecular Predissociation

B. R. Lewis and S. T. Gibson

Research School of Physical Sciences and Engineering, The Australian National University, Canberra, ACT 0200, Australia

P. O'Keeffe,* T. Ridley, K. P. Lawley, and R. J. Donovan

Department of Chemistry, The University of Edinburgh, West Mains Road, Edinburgh EH9 3JJ, United Kingdom

(Received 23 August 2000)

A unique observation is presented of interacting predissociating resonances which exhibit completely destructive interference in a region between the resonances. The use of a double-resonance technique, in which single rotational levels of the $b\ ^1\Sigma_g^+$ state of O_2 , prepared by pumping the magnetic-dipole $b \leftarrow X$ transition, are probed by (2 + 1) resonance-enhanced multiphoton-ionization spectroscopy, eliminates overlapping rotational structure and enables observation of the interference process. Using a diabatic coupled-channel model, the interacting resonances are shown to be derived from the $d\ ^1\Pi_g(v = 3, J = 17)$ Rydberg and $11\ ^1\Delta_g(v = 6, J = 17)$ valence states.

DOI: 10.1103/PhysRevLett.86.1478

PACS numbers: 33.70.Jg, 33.80.Gj, 33.40.+f, 33.80.Rv

Resonant phenomena are commonplace in many branches of physics, e.g., nuclear reactions, electron scattering from atoms and molecules, atomic and molecular photoionization and photodetachment, and molecular photodissociation. Quantum-interference effects between resonances may occur in certain cases where their separation is comparable to their widths. Several different, but complementary, theoretical techniques have been employed in the treatment of such interacting resonances, e.g., configuration-interaction (CI) theory [1,2], originally applied to autoionizing Rydberg series, the K -matrix formalism [3], first developed to describe nuclear scattering, and multichannel quantum-defect theory [4], particularly suited to the concise description of complex interactions in autoionization [5] and predissociation [6].

While there have been many complex examples of interacting resonances reported in the literature for most of the above fields (see, e.g., the review by Connerade and Lane [3] for atomic autoionization), there have been very few experimental observations which demonstrate the simple cases first studied theoretically by Fano [1] and Mies [2]. In particular, examples of the completely destructive quantum interference predicted for certain interactions are minimal, presumably because of the inherent multichannel character of most resonant interactions, together with the effective "filling in" of interference minima by limited experimental resolution, incoherent continua, or other incoherent structures.

Local perturbations in molecular predissociation should provide an ideal opportunity to observe two-resonance interactions in detail, but such observations will normally be hampered by the effects of incoherent overlapping structure. Only two convincing examples of interacting resonances have been reported for molecular predissociation below the first ionization limit, resulting from photofragment [7] and photoabsorption [8] spectroscopies, but, in

both cases, the measurements were limited by the presence of unresolved rotational structure.

In this Letter, we report a unique observation of interacting predissociating resonances in O_2 which exhibit completely destructive interference in a region between the resonances. Observation of the interference effect was made possible, free from the obscuring effects of limited instrumental resolution and incoherent overlapping rotational structure, by the use of a high-resolution, rotationally selective, optical-optical double-resonance (OODR) experimental technique, together with ionization detection.

The experimental details have been discussed elsewhere [9]. Briefly, the $b\ ^1\Sigma_g^+ \leftarrow X\ ^3\Sigma_g^-(0,0)$ magnetic-dipole transition of O_2 near 760 nm was excited by a Ti:sapphire laser pumped by the second harmonic of a Nd:YAG laser. The laser produced 25 mJ pulses of 8–9 ns duration, at a repetition rate of 5 Hz, and with a bandwidth of $\sim 0.4\text{ cm}^{-1}$ full width at half maximum (FWHM). After a delay of 50–100 ns, the resultant $b(v = 0, J)$ levels selectively excited in this way were probed by an excimer-pumped dye laser, operating near 340 nm with the dye p-Terphenyl, via a two-photon transition to the Rydberg $d\ ^1\Pi_g(v = 3)$ state. The wavelength of the probe laser (bandwidth $\sim 0.2\text{ cm}^{-1}$ FWHM) was calibrated against the neon optical galvanic spectrum, resulting in an overall absolute uncertainty of $\sim 0.5\text{ cm}^{-1}$ in the transition energy. The counterpropagating pump and probe laser beams were focused to an overlapping point in a differentially pumped ionization chamber and intersected at 90° by a pulsed molecular beam of O_2 . The resultant O_2^+ ions were collected by a time-of-flight mass spectrometer and the ion current from the microchannel-plate detector was processed by a boxcar integrator.

Diabatic potential-energy curves for the *gerade* electronic states of O_2 relevant here are shown in Fig. 1, together with the OODR and ionization pathways. Although

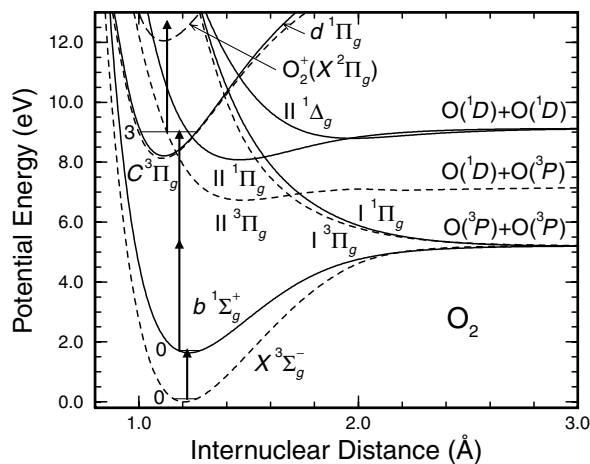


FIG. 1. Diabatic potential-energy curves for *gerade* electronic states of O_2 relevant to the present study (solid curves: singlets; dashed curves: triplets). The OODR excitation scheme, $d^1\Pi_g(v=3) \leftarrow b^1\Sigma_g^+(v=0) \leftarrow X^3\Sigma_g^-(v=0)$, and subsequent detection by ionization into low vibrational levels of $O_2^+(X^2\Pi_g)$ (long-dashed curve), are also indicated.

the $b \leftarrow X$ transition is electric-dipole forbidden, it does have a weak magnetic-dipole transition moment which allows efficient pumping by high-power lasers [9,10]. In the present case, the P -branch magnetic-dipole transitions were used to pump even- J levels of the b state, the odd- J levels for the homonuclear $^{16}O_2$ being nonexistent due to nuclear-spin statistics. Subsequently, these $b(v=0, J)$ levels were probed by $(2+1)$ resonance-enhanced multiphoton-ionization (REMPI) spectroscopy via the $d(v=3)$ state [11], leading to observed spectra containing only the single O -, P -, Q -, R -, and S -branch lines allowed by the two-photon selection rules [12]. Vibrational levels of the d state are broadened due to indirect predissociation by the $I^1\Pi_g$, $I^3\Pi_g$, and $II^3\Pi_g$ valence states [13,14] (see Fig. 1). Overall $(2+1)$ -REMPI spectra resulting from the probing of the $J=0$ to 16 rotational levels of $b(v=0)$ have been reported elsewhere [9]. Despite strong perturbations caused by Rydberg-valence interactions between the bound $d^1\Pi_g$ and $II^1\Pi_g$ states [14] (see Fig. 1), the accessed rotational levels of $d(v=3)$ were found to have roughly constant predissociation widths of $3.5 \pm 1 \text{ cm}^{-1}$ FWHM [9].

Here, we are concerned specifically with $d(v=3, J=17)$. Our experimental $d^1\Pi_g(v=3, J=17) \leftarrow b^1\Sigma_g^+(v=0, J=16)$ $(2+1)$ -REMPI spectrum is shown in detail in Fig. 2 (solid circles). Rather than the single $d(v=3) \leftarrow b(v=0)R(16)$ predissociating resonance with FWHM $\sim 3.5 \text{ cm}^{-1}$ that might have been expected in this energy region, two narrower resonances appear. This doubling of $d(v=3, J=17)$ has been noted only recently [14] and attributed to a weak local perturbation caused by interaction between the $d^1\Pi_g$ Rydberg and weakly bound $II^1\Delta_g$ valence states, indirectly, via the $II^1\Pi_g$ valence state (see Fig. 1).

In addition to the energy and width anomalies associated with this local perturbation, the experimental spectrum of

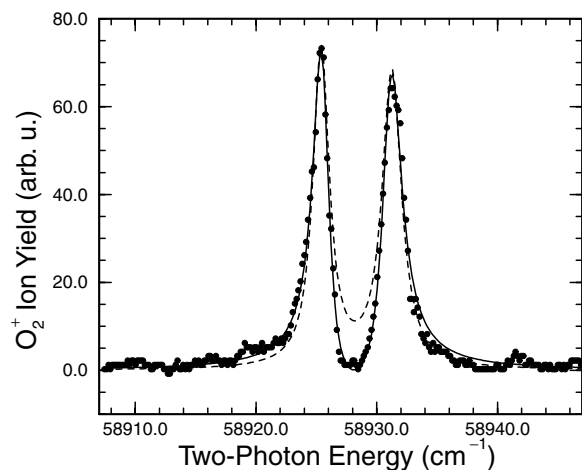


FIG. 2. Closely interacting predissociating resonances in the $(2+1)$ -REMPI spectrum of O_2 excited from $b^1\Sigma_g^+(v=0, J=16)$. The upper- and lower-energy resonances correspond to $R(16)$ transitions into the interacting Rydberg $3s\sigma_g d^1\Pi_g(v=3, J=17)$ and valence $II^1\Delta_g(v=6, J=17)$ levels, respectively. The experimental spectrum (solid circles) displays a region of completely destructive quantum interference between the resonances, which is in good agreement with a fitted model of interacting resonances based on the Fano theory [Eq. (1)] (solid curve), but differs dramatically from expectation for noninteracting resonances (dashed curve).

Fig. 2 displays the unmistakable signature of quantum interference between interacting resonances. While the outer wings of the resonances are prominent, in the energy region between the resonances the ion signal rapidly reaches the background level. This unique experimental result is, effectively, a textbook example of the two-discrete-state, one-(inactive)-continuum case of interacting resonances treated many years ago by Fano [1] and Mies [2], using CI theory. The observation in Fig. 2 corresponds to the specific “maximum-overlap” case of Mies [2], exhibiting completely destructive interference at an energy between the resonances. The line shape for this case can be written as [1–3,15]

$$\sigma(\nu) \propto \frac{(\frac{\Gamma_1/2}{\nu-\nu_1} + r \frac{\Gamma_2/2}{\nu-\nu_2})^2}{1 + (\frac{\Gamma_1/2}{\nu-\nu_1} + \frac{\Gamma_2/2}{\nu-\nu_2})^2}, \quad (1)$$

where the Γ_i and ν_i are the resonance widths and energies, respectively, and r is a relative amplitude factor, which, in the present case, also includes such factors as differences in the relative ionization efficiencies of the two resonances, labeled 1 and 2, respectively, in order of increasing energy. The result of a least-squares fit of Eq. (1) to the experimental spectrum is shown in Fig. 2 as a solid curve [16]. There is good agreement between the fit and the measurements, confirming the appropriateness of the interacting-resonances picture embodied in Eq. (1). The resulting resonance parameters are $\Gamma_1 = 1.53 \pm 0.03 \text{ cm}^{-1}$ FWHM, $\Gamma_2 = 1.86 \pm 0.04 \text{ cm}^{-1}$ FWHM, $\nu_1 = 58925.39 \pm 0.02 \text{ cm}^{-1}$, $\nu_2 = 58931.25 \pm 0.02 \text{ cm}^{-1}$, and $r = 0.958 \pm 0.010$. On the other hand, a profile generated using the same resonance parameters, but assuming

independent resonances [17], shown as a dashed curve in Fig. 2, is in poor agreement with the measurements, falling only to $\sim 15\%$ of the peak resonance height in the region between the resonances. Thus, the magnitude of the destructive interference effect is confirmed.

The resonances displayed in Fig. 2 may be viewed naively as arising from a simple two-level interaction [18]. Almost coincident “adiabatic” levels, only one of which is predissociated and has significant intensity in transitions from the initial state, mix nearly completely, with an effective interaction matrix element $H_{12} = 2.92 \pm 0.06 \text{ cm}^{-1}$, resulting in resonances of roughly equal intensity and predissociation linewidth. This picture is consistent with the suggested assignment of the perturber of the $d^1\Pi_g$ state to the $\Pi^1\Delta_g$ state [9,14], which has a large equilibrium internuclear separation ($R_e \approx 2.0 \text{ \AA}$; see Fig. 1), making it unlikely to be crossed and predissociated by repulsive states correlating with lower dissociation limits, and resulting in a negligible Franck-Condon overlap factor (FCF) with the $b^1\Sigma_g^+$ state ($R_e \approx 1.2 \text{ \AA}$), and thus zero intensity in two-photon transitions from this state. The fact that the sum of the fitted linewidths, $\Gamma_1 + \Gamma_2 \approx 3.4 \text{ cm}^{-1}$ FWHM, is essentially equal to the expected unperturbed width for $d(\nu = 3, J = 17)$ also supports this interpretation.

However, the simplicity of the foregoing behavior and analysis belies the complexity of the actual adiabatic-basis interactions leading to the perturbation and predissociation of the d state, which are summarized schematically in Fig. 3. In fact, the $d^1\Pi_g$ and $\Pi^1\Delta_g$ states interact indirectly via many levels of the $\Pi^1\Pi_g$ state. The $d^1\Pi_{1g}$ and $\Pi^1\Pi_{1g}$ states interact strongly electrostatically (H^{el}), while the $\Pi^1\Pi_{1g}$ and $\Pi^1\Delta_{2g}$ states exhibit a weak rotational interaction (H^{JL}) [14,19]. The $\Pi^1\Pi_{1g}$ state undergoes direct predissociation through an electrostatic interaction with the $1^1\Pi_{1g}$ -state continuum, while the

$d^1\Pi_{1g}$ state is indirectly predissociated by the $1, \Pi^3\Pi_{1g}$ continua due to spin-orbit (H^{SO}) and electrostatic interactions. Two-photon transitions are allowed from the $b^1\Sigma_g^+$ state to the $1^1\Pi_{1g}$ and $\Pi^1\Delta_{2g}$ states, but we consider only the $d \leftarrow b$ and $\Pi^1\Pi_g \leftarrow b$ transitions (electronic transition moments D_R and D_V , respectively), since FCFs for the remainder are negligible. Thus, there is no optically active continuum involved.

These multilevel interactions are treated most conveniently using coupled-channel (CC) computational techniques [20]. Application of the CC method to the coupled $1,3\Pi_{1g}$ states of O_2 in Fig. 3 has been described in detail by Lewis *et al.* [14]. Our adiabatic CC model is based on that of Ref. [14], with further optimization of the $1^1\Pi_g$ potentials and couplings to take account of the new experimental d -state linewidths and energies determined by O’Keeffe *et al.* [9]. In addition, here we include the $\Pi^1\Delta_g$ state specifically in the model CC basis. The model potential-energy curves employed are those shown in Fig. 1. The $1^1\Pi_g$ potentials differ only through small shifts in internuclear distance and/or energy from those in Ref. [14], while the $\Pi^1\Delta_g$ potential is based on the multireference CI calculation of Partridge [21], shifted up by $\sim 15 \text{ cm}^{-1}$ to match the expected unperturbed energy for $\nu = 6, J = 17$. The electronic couplings are those of Ref. [14], except that the $1^1\Pi_g$ Rydberg-valence coupling is 620 cm^{-1} (630 in Ref. [14]), and the $1^1\Pi_g$ valence-valence coupling is 420 cm^{-1} (500 in Ref. [14]). Finally, the electronic part of the rotational interaction between the $\Pi^1\Pi_{1g}$ and $\Pi^1\Delta_{2g}$ states is 2.8 cm^{-1} , this value being necessary to best reproduce the observed behavior of the interacting resonances in Fig. 2.

Two-photon photodissociation cross sections for excitation from $b^1\Sigma_g^+(\nu = 0, J = 16)$ to the coupled states with $J = 17$ in the region of the interacting resonances, calculated using our CC model, are compared with our “experimental” results in Fig. 4. Assuming that the ionization step is saturated, and that predissociation dominates the competition with ionization, the REMPI spectrum of Fig. 2 has been converted into an effective dissociation spectrum by scaling the intensities of the resonances by their widths [14]. Thus, the open circles in Fig. 4 were determined using Eq. (1) with the experimental resonance parameters, but now with $r = 1.056$. The CC spectrum calculated assuming $D_R \neq 0$ and $D_V = 0$ (solid curve) is in excellent agreement with experiment, unlike that calculated with $D_R = 0$ and $D_V \neq 0$ (long-dashed curve), suggesting that the Rydberg excitation plays the dominant role in the two-photon process. We have also performed comparable calculations following removal of the $\Pi^1\Delta_g$ perturbing state from the CC basis. The results, shown as dashed and dot-dashed curves in Fig. 4, for principally Rydberg and valence excitation, respectively, are consistent with expectation for an unperturbed Lorentzian resonance associated with $d(\nu = 3)$.

Thus, surprisingly, despite the complexity of the multilevel interactions embodied in Fig. 3, the CC results for

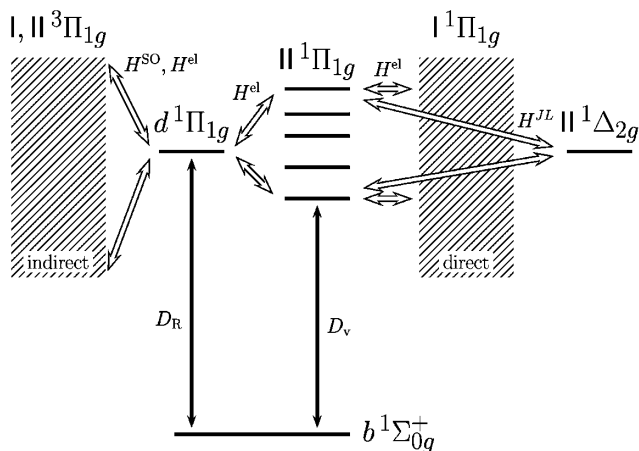


FIG. 3. Schematic diabatic-level representation of the coupled *gerade* states of O_2 accessed at the two-photon level in the current excitation scheme. Two-photon electronic transition pathways are indicated by single lines, electronic couplings by double lines.

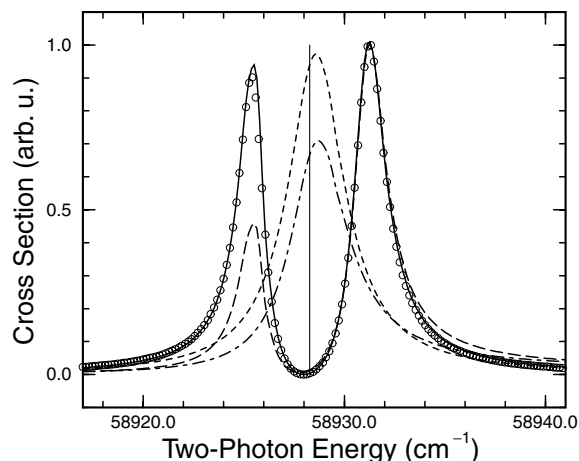


FIG. 4. Comparison between experimental and CC two-photon photodissociation spectra for the perturbed $d^1\Pi_g(v=3, J=17) \leftarrow\leftarrow b^1\Sigma_g^+(v=0, J=16)$ transition of O_2 . Open circles: from fit to experimental (2 + 1)-REMPI spectrum of Fig. 2, corrected for competition between predissociation and ionization. Solid and short-dashed curves: computed spectra, assuming preferential excitation of the diabatic $d^1\Pi_g$ Rydberg state, for the full CC model, and a reduced model lacking the $\Pi^1\Delta_g$ channel, respectively. Long-dashed and dot-dashed curves: as above, but assuming preferential excitation of the diabatic $\Pi^1\Pi_g$ valence state. The computed energy of the unperturbed $\Pi^1\Delta_g(v=6, J=17) \leftarrow\leftarrow b^1\Sigma_g^+(v=0, J=16)$ transition is indicated by the vertical line. All computed spectra have been shifted by $+0.9\text{ cm}^{-1}$ in energy and scaled to a peak height of unity for the right-hand resonance, for better comparison with experiment.

Rydberg excitation are consistent with the simple two-level picture suggested by the observations. This can be understood by considering the strong $d^1\Pi_g \sim \Pi^1\Pi_g$ level interactions to be *prediagonalized*, resulting in a broad Rydberg level $d(v=3, J=17)$ which has significant $\Pi^1\Pi_g$ valence character. Because of an *accidental energy degeneracy*, the pure $\Pi^1\Delta_g(v=6, J=17)$ level interacts significantly only with this d -state level [22], the interaction occurring through the valence admixture in the Rydberg wave function. Thus, effectively, we have the situation treated using CI theory by Lewis *et al.* [8], where a narrow, dark level is predissociated indirectly by a broad, bright, degenerate level, resulting in simple width and strength sharing, and destructive interference in the cross section described by Eq. (1). However, the destructive interference in the observation reported by Lewis *et al.* [8] was obscured by other rotational structure. In other fields, as far as we are aware, only nuclear scattering provides examples of any comparability. For example, Callender and Browne [23] report a nearly complete destructive interference between two resonances, but with a strong incoherent continuous background.

The authors thank Professor A.R.P. Rau and Dr. K.G.H. Baldwin for critical comments.

*Present address: Physical and Theoretical Chemistry Laboratory, South Parks Road, Oxford OX1 3QZ, United Kingdom.

- [1] U. Fano, Phys. Rev. **124**, 1866 (1961).
- [2] F.H. Mies, Phys. Rev. **175**, 164 (1968).
- [3] J.-P. Connerade and A.M. Lane, Rep. Prog. Phys. **51**, 1439 (1988), and references therein.
- [4] M.J. Seaton, Rep. Prog. Phys. **46**, 167 (1983); C.H. Greene and Ch. Jungen, Adv. At. Mol. Phys. **21**, 51 (1985); U. Fano and A.R.P. Rau, *Atomic Collisions and Spectra* (Academic, Orlando, FL, 1986).
- [5] A. Giusti-Suzor and H. Lefebvre-Brion, Phys. Rev. A **30**, 3057 (1984).
- [6] F.H. Mies, J. Chem. Phys. **80**, 2514 (1984); F.H. Mies and P.S. Julienne, *ibid.* **80**, 2526 (1984).
- [7] B. Kim, K. Yoshihara, and S. Lee, Phys. Rev. Lett. **73**, 424 (1994).
- [8] B.R. Lewis *et al.*, Phys. Rev. A **55**, 4164 (1997).
- [9] P. O’Keeffe *et al.*, J. Chem. Phys. **113**, 2182 (2000).
- [10] A. T.J.B. Eppink *et al.*, J. Chem. Phys. **108**, 1305 (1998).
- [11] A similar OODR scheme, via $b(v=1,2)$, has been used by H.I. Bloemink, R.A. Copeland, and T.G. Slinger, J. Chem. Phys. **109**, 4237 (1998).
- [12] R.G. Bray and R.M. Hochstrasser, Mol. Phys. **31**, 412 (1975).
- [13] J.S. Morrill, M.L. Ginter, B.R. Lewis, and S.T. Gibson, J. Chem. Phys. **111**, 173 (1999).
- [14] B.R. Lewis, S.T. Gibson, J.S. Morrill, and M.L. Ginter, J. Chem. Phys. **111**, 186 (1999).
- [15] Equation (1) is appropriate for an optically inactive continuum. The expression for an active continuum [e.g., Eq. (50) of Ref. [2]] contains Fano asymmetry parameters for each resonance.
- [16] Convolution with a Gaussian instrumental function of 0.3 cm^{-1} FWHM was included in the fitting procedure, but the resonance parameters were not very sensitive to this bandwidth. The Doppler width was insignificant.
- [17] In the language of nuclear physics, the solid curve [Eq. (1)] represents a “coupled Breit-Wigner” profile, the dashed curve the sum of two noninterfering Breit-Wigner (Lorentzian) terms.
- [18] H. Lefebvre-Brion and R.W. Field, *Perturbations in the Spectra of Diatomic Molecules* (Academic, Orlando, FL, 1986), pp. 247–248.
- [19] Numerical subscripts in the electronic-state designations represent the values of Ω .
- [20] E.F. van Dishoeck, M.C. van Hemert, A.C. Allison, and A. Dalgarno, J. Chem. Phys. **81**, 5709 (1984).
- [21] H. Partridge (private communication); H. Partridge, C.W. Bauschlicher, Jr., S.R. Langhoff, and P.R. Taylor, J. Chem. Phys. **95**, 8292 (1991).
- [22] The $\Pi^1\Delta_g(v=6, J=17)$ level interacts weakly with other mixed Rydberg-valence $^1\Pi_g$ levels, but the corresponding wave function admixtures are negligible due to the comparative energetic remoteness of those levels.
- [23] W.D. Callender and C.P. Browne, Phys. Rev. C **2**, 1 (1970).